Extravalence molecular excitations in inert matrices

Aharon Gedanken, Baruch Raz, and Joshua Jortner
Department of Chemistry, Tel-Aviv University, Tel-Aviv, Israel
(Received 24 July 1972)

In this paper we present the results of an experimental study of extravalence excitations of molecular impurities in solid rare gases and in molecular host matrices. We report the absorption spectra of methyl iodide, benzene, ethylene, and acetylene in solid Ne, Ar, Kr, Xe, N_2, and CF_4 in the spectral region 2000–1150 Å. Spectroscopic evidence has been obtained for the observation of high ($n \geq 2$) Wannier impurity states originating from a molecular positive ion. These molecular Wannier series yield spectroscopic information concerning the energetics of molecular photoionization in a dense medium. The large blue spectral shifts of the lowest extravalence molecular excitations in dense media can be rationalized in terms of central cell corrections to the $n=1$ Wannier state, which are determined by the exciton binding energy.

I. INTRODUCTION

Recent experimental and theoretical studies have established that the lowest extravalence excitations of atomic and molecular impurities in rare gas solids and in some molecular matrices are amenable to experimental observation.[1–4] Conclusive experimental evidence has been obtained for the identification of the lowest Rydberg states of acetylene,[5] ethylene,[6,7] benzene,[6,7] naphthalene,[8] carbon disulphide,[9] and carbon oxysulphide[9] in low temperature rare gas matrices and of acetylene and methyl iodide in solid CF_4.[10] It is well known that when the impurity binding energy is small relative to the band gap of the host matrix the Wannier model constitutes a proper description of the physical situation, and this approach has been very successful in the interpretation of shallow impurity states.[11] For deep impurity states pseudopotential theory was utilized to rationalize the observation of Wannier states.[12] Both shallow and deep highly excited impurity states can be described in terms of the well known effective mass equation. When the conduction band is parabolic, the highly excited impurity energy levels E_n, as described by a hydrogenic series

$$E_n = E_G - G/n^2 \tag{1}$$

with

$$G = 13.6(m^*/\mathcal{K}^2)\ \text{eV} \tag{2}$$

converging to the bottom of the conduction band. Here m^* is the electron effective mass (in the conduction band), $\mathcal{K}$ represents the static dielectric constant, while E_G corresponds to the impurity energy gap, which is given by

$$E_G = I_g + P_+ + V_0, \tag{3}$$

where I_g is the impurity gas phase ionization potential, P_+ is the medium polarization energy by the impurity positive ion and V_0 is the energy of the bottom of the matrix conduction band (relative to the vacuum level).

The lowest extravalence impurity excitation in simple molecular solids (corresponding to the $n=1$ state) cannot be adequately described in terms of the Wannier model [Eq. (1)], as the overlap of this excited state, with the medium, is not sufficiently large to make the effective mass approximation valid, to justify the macroscopic dielectric screening approximation and to neglect the repulsive electron hole interactions.[13] Thus, the Wannier scheme has to be modified by the introduction of appreciable central cell corrections.[12] The application of pseudopotential theory[12] indicates that the energy $E_{(1)}$ of this state can be recast in the form of

$$E_{(1)} = E_1 + \Delta E_c, \tag{4}$$

where E_1 is given by Eq. (1) while the central cell correction ΔE_c consists of three major contributions[12]

$$\Delta E_c = E_m + E_D + E_R, \tag{5}$$

where E_m is the correction to the effective mass and E_D corresponds to the contribution of the effects of spatial dispersion (i.e., the distance from the positive ion core). The calculations of Hermanson and Phillips[12] demonstrate that ΔE_c is a monotonic increasing function of the exciton binding energy, G. This correlation has been recently confirmed for Xe impurity in a large number of atomic and molecular host matrices.[10]

An alternative description of this lowest extravalence excitation in a dense medium involves the modified tight binding scheme. Here the energy shift of the lowest molecular Rydberg state (relative to the gas phase value) originates from a delicate balance between repulsive nonorthogonality interactions (resulting in large positive energy corrections) and between charge transfer and dispersion interactions (leading to negative energy corrections).[14] From the experimental point of view the lowest extravalence excitation of an atomic or molecular impurity in rare gas solids[1–8] and in solid CF_4,[10] exhibits an appreciable blue spectral shift relative to the gas phase value indicating the

dominating role of short range repulsive interactions. It is, however, very difficult to adopt the modified tight binding scheme for a quantitative interpretation of these spectral shifts. From the theoretical point of view, the modified Wannier scheme[12] is more suitable for the semiquantitative rationalization of the location of the $n=1$ intermediate excited state.

Higher extravalence excitations of an impurity molecule in a matrix are not expected to reveal any relation to the corresponding molecular states in the gas phase, and should be adequately described in terms of the Wannier model [Eq. (1)]. It is still an open question whether these $n=2$ higher excited states, originating from a molecular positive ion, are amenable to experimental detection. Katz *et al.*[6] have provided a tentative identification of the $n=2$ state for benzene in solid Kr and in Xe, while no higher members of the Wannier series were identified. Some evidence for the observation of the higher members of a Wannier series was presented by Angus and Morris[8] for naphthalene in solid Ar, Kr, and Xe. The interpretation of these spectroscopic data raises some problems, as the identification of the $n=1$ member of the Wannier series is inconclusive,[8] the matrix shifts obtained for the lowest extravalence excitation follow an irregular pattern, and the intensity ratio between the $n=1$ and the $n=2$ series members seems to be smaller than unity in contrast to theoretical predictions.

In this work we present the results of an experimental study of the extravalence excitations of methyl iodide, ethylene, acetylene, and benzene in rare gas solids (Ne, Ar, Kr, and Xe) and in molecular host matrices (solid CF_4 and solid N_2). We have chosen a number of molecular impurities which exhibit different features of the positive ion core. Our data provide new information concerning the features of molecular Wannier impurity states in monoatomic (i.e., rare gas) and in molecular (solid CF_4 and solid N_2) host matrices.

II. EXPERIMENTAL METHODS

A. Spectrograph and Light Sources

A 1-m normal incidence vacuum ultraviolet monochromator (McPherson 225) with a resolution of ~3 Å was used. The spectral region 1150–1900 Å was scanned using a modified version of the Tanaka, Ar, Kr, and Xe molecular continuum discharge lamps.[15] Single beam photoelectric detection was employed utilizing an EMI 9514S photomultiplier and a sodium salicylate converter. All our experimental data (except the preliminary experiments reported in Sec. II.D) were obtained applying the converter on the front window of the photomultiplier.

B. Cryostat

The solid samples were prepared by injecting the gaseous mixtures on a cooled LiF window. This window was mounted on a helium flow cryostat described in Fig. 1 (designed jointly with Ricor Ltd.). The liquid helium consumption of this cryostat was 1.5 liter per h, being proportional to the operation duration. The temperature measurements were performed by attaching a Chromel vs gold-iron thermocouple to the LiF window mounted on the cryostat. The lowest temperature attainable in this cryostat was 6 ± 2°K. The temperature could be continuously varied in the range 6–100°K and kept constant within ±0.5°K. Temperature control was achieved by the use of two needle valves regulating the helium flow through the exit of the cryostat.

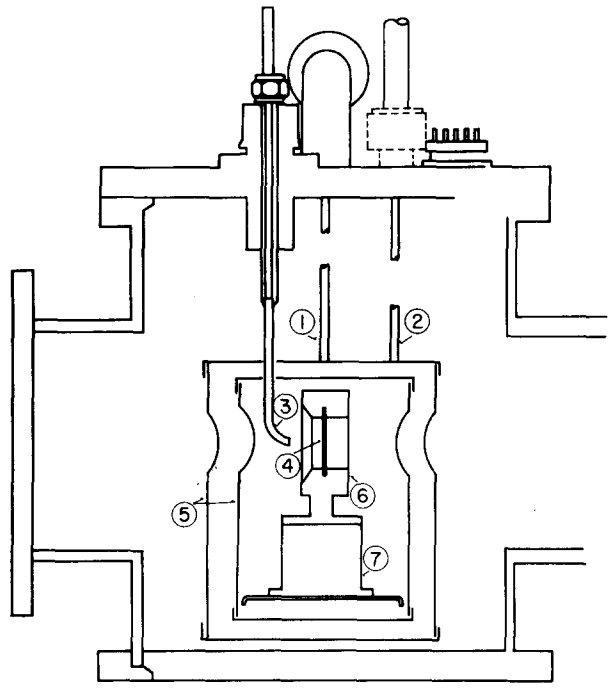

FIG. 1. A schematic diagram of the helium flow cryostat: 1. helium inlet, 2. helium outlet, 3. movable injection nozzle, 4. LiF window, 5. radiation shields, 6. window holder, 7. heat exchanger.

The gaseous mixtures were injected through an injection nozzle onto the cold window. After completing the injection stage, the nozzle could be removed from the light path. Throughout the injection, the temperature of the nozzle was kept at 300°K, by a thermocoax heater placed around the tip of the injection pipe.

We have checked the amount of stray light introduced by the reflecting surfaces of the gold coated radiation shields of the cryostat. This was done by masking the rear side of the LiF window with a black tape and measuring the photomultiplier signal. The stray light thus measured was ~0.2% so that our measurements were limited up to optical density of 2.0.

C. Sample Preparation

Matheson research grade rare gases, nitrogen and carbon tetrafluoride were used for the production of

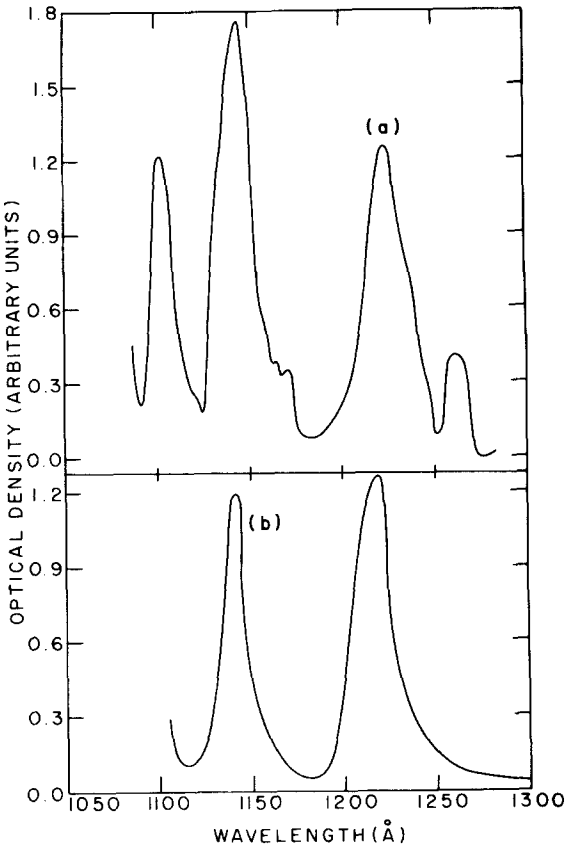

FIG. 2. (a) Absorption spectrum of solid krypton, deposited on a sapphire window coated with sodium salicylate converter (at 30°K). (b) Absorption spectrum of solid krypton, deposited on a LiF window at 30°K.

the host matrices. The impurity molecules were of high chemical purity (~99%), and in view of their low concentration no further purification was required.

The gaseous mixtures containing 0.05%–1% of the impurity molecule were prepared in a vacuum system which was pumped to an initial pressure of less than 10^{-6} torr. The gaseous mixture was then injected onto the cooled LiF window, where the measured pressure in the spectrograph chamber prior to the injection was 2×10^{-7} torr. Ne matrices were deposited and measured at 6±2°K, while Ar, Kr, Xe, CF_4, and N_2 matrices were prepared and measured in the temperature range 10–30°K. We have observed an appreciable enrichment of the solid samples of (organic molecules)/Ne and of Xe/Ne (deposited at 6±2°K) relative to the gas phase composition, the enrichment factor for the impurity was ~10. Thus the gaseous mixtures used for the study of Ne matrices were prepared to contain 0.05%–0.1% of the impurity molecule. Argon and N_2 matrices (deposited at 20°K) exhibited an enrichment factor of ~2, while no enrichment of the solid matrix relative to the gas phase composition is expected for Kr and for Xe matrices. The argon and nitrogen gaseous mixtures were doped with ~0.3%–0.5% of the impurity molecule, while xenon and CF_4 gaseous mixtures were prepared at the doping level of 1%. All our solid samples contained about ~1% of the impurity molecule.

The purity of the host matrices and of our gas handling procedure was checked by measurements of the transmission of pure films (~0.1 μ thickness) of Ne, Ar, Kr, Xe, and CF_4. Solid Ne and CF_4 were found to be transparent down to 1100 Å (the cutoff of our spectroscopic system), while the absorption onsets in the other host matrices were as follows: 1100 Å for Ar, 1300 Å for Kr, 1550 Å for Xe, and 1500 Å for N_2. No weak parasitic absorption lines were observed in the transparency region of these matrices.

D. Spectra of Pure Rare Gases

We have performed some control experiments mounting on the cryostat a sapphire window coated by a sodium salicylate converter. This is essentially the technique originally introduced by Baldini who employed the Liumogen converter.[16] The gross features of the spectra of pure rare gas films (~100–200 Å thickness) deposited on the coated sapphire coated window (Fig. 2) are in good agreement with Baldini's original results.[16] However, our spectra exhibit an additional absorption peak at 1252 Å in solid Kr and at 1510 Å in solid Xe. This peak has been reported by several groups and has been referred to as "Peak A".[17] On the other hand, some other investigators have failed to observe this absorption band.[18,1]

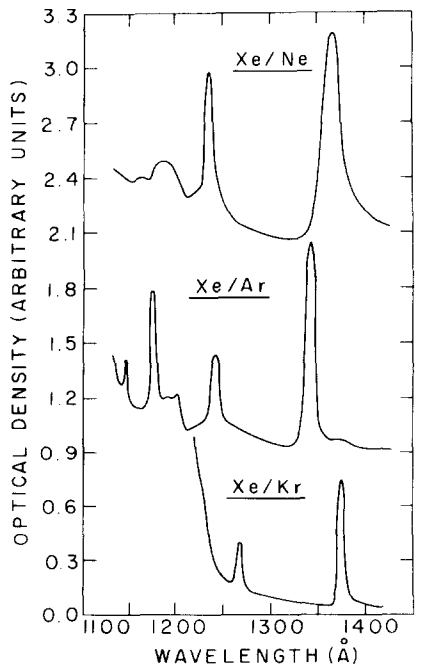

FIG. 3. Absorption spectra of solid rare gas alloys. The gas phase concentrations were: 0.02% Xe in Ne, 0.1% Xe in Ar, 0.1% Xe in Kr. Deposition temperatures: 6°±2°K for Xe/Ne, 20°K for Xe/Ar, and 30°K for Xe/Kr.

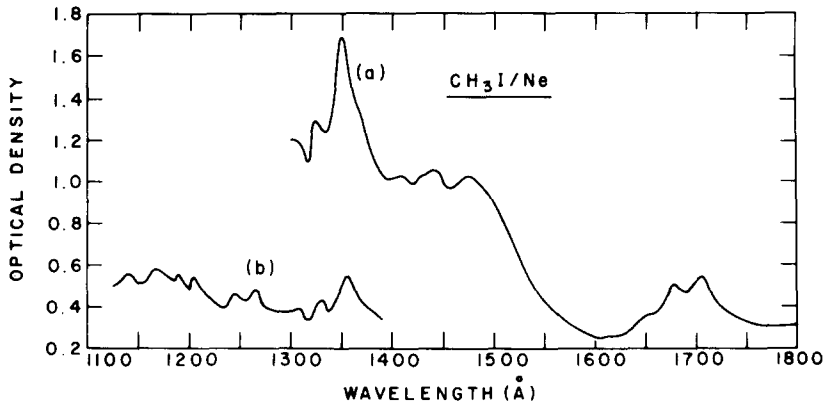

FIG. 4. Absorption spectrum of CH_3I in solid Ne. Gas phase composition 0.01% CH_3I in Ne. Deposition temperature 6°±2°K. Curve (a), xenon continuum and krypton continuum light source. Curve (b), argon continuum light source.

In a series of experiments designed to reproduce the spectra of rare gas alloys we have obtained results indicating a considerable temperature gradient on the sodium salicylate converter layer. We have then replaced the coated sapphire window by a LiF (1 mm thick) window and coated the photomultiplier by the converter. The lower temperature of the front surface of the LiF substrate resulted in the disappearance of "Peak A" (see Fig. 2). The disappearance of "Peak A" in samples deposited on LiF indicates that this peak is not a trivial site effect and that its appearance depends on the structure of the deposited film. A tentative assignment of this absorption involved the $^1S_0 \rightarrow {}^3P_2$ transition, which becomes allowed due to a low symmetry crystal field. The separation of the "Peak A" and the strong $^1S_0 \rightarrow {}^3P_1$ transition in solid Xe and Kr corresponds quite well to the splitting of the Xe and Kr $^3P_2$ and $^3P_1$ atomic terms. However, at present we cannot exclude the possibility that "Peak A" is due to a surface state.

E. Rare Gas Alloys

As a final control experiment, we have used a LiF window and measured the absorption spectra of rare gas alloys (film thickness 0.1–1 μ). These spectra (Fig. 3) are in good agreement with Baldini's original results.[1]

III. EXPERIMENTAL RESULTS

A. Methyl Iodide Impurity States

A substantial amount of experimental and theoretical work on deep impurity states in rare gas solids has been performed using Xe as a typical impurity atom.[1,14,4,10] It seemed to us natural to investigate the impurity states of methyl iodide in atomic and molecular host matrices, as the lowest extravalence excitations of this molecule are isoelectronic with the Xe atomic $^1S_0 \rightarrow {}^3P_1$ and $^1S_0 \rightarrow {}^1P_1$ transitions. The first Rydberg state of CH_3I in the gas phase originates from the I atom $5p \rightarrow 6s$ transition, the CH_3I^+ core being in the $^2E_{3/2}$ or $^2E_{1/2}$ state.[19] In the matrix we expect two Wannier series $n(^2E_{3/2})$ and $n(^2E_{1/2})$, where the lower members of the two series are split by the iodine atom spin orbit splitting (0.595 eV in the gas phase spectrum of CH_3I).[19] As in the case of the Xe atomic impurity the spin orbit coupling in the matrix may be somewhat modified due to nonorthogonality

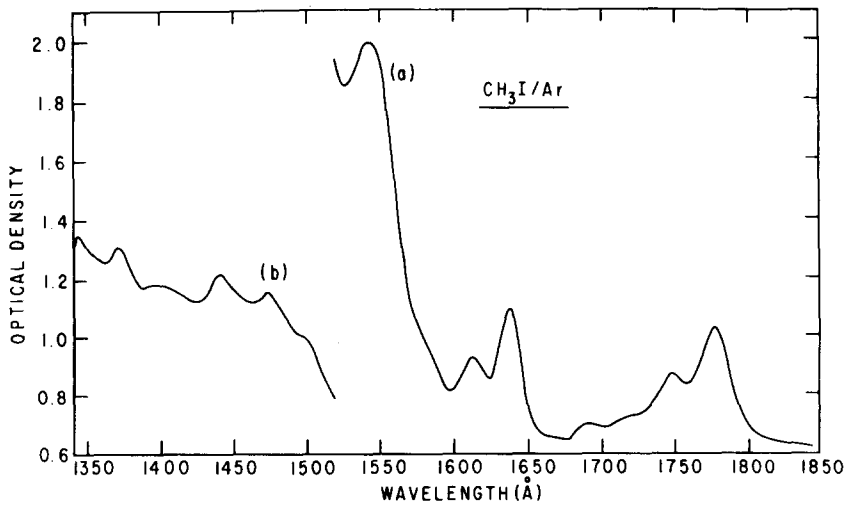

FIG. 5. Absorption spectrum of CH_3I in solid Ar. Gas phase composition 0.5% CH_3I in Ar. Deposition temperature 20°K. Curve (a) xenon continuum light source. Curve (b) krypton continuum light source.

TABLE I. Energy levels of CH_3I impurity states in solid matrices.

Neon		Argon		Krypton		CF_4		
Wavelength Å	Energy cm^{-1}	Wavelength Å	Energy cm^{-1}	Wavelength Å	Energy cm^{-1}	Wavelength Å	Energy cm^{-1}	Assignment
1705	58 650	1780	56 180	1825	54 795	1598	62 580	$n=1(^2E_{3/2})$
1677	59 630	1750	57 140	1792	55 800			$n=1(^2E_{3/2})+\nu_2$
1655	60 420	1723	58 040	1748	57 210			$n=1(^2E_{3/2})+2\nu_2$
		1695	59 000					$n=1(^2E_{3/2})+3\nu_2$
1352	73 965	1640	60 975	1680	59 520	1455	68 730	$n=1(^2E_{1/2})$
1326	75 415	1615	61 920	1650	60 610			$n=1(^2E_{1/2})+\nu_2$
1305	76 630							$n=1(^2E_{1/2})+2\nu_2$
1475	67 800	1542	64 725	1635	61 160			$n=2(^2E_{3/2})$
1441	69 400			1605	62 305			$n=2(^2E_{3/2})+\nu_2$
1410	70 920							$n=2(^2E_{3/2})+2\nu_2$
		1495	66 890	1570	63 695			$n=3(^2E_{3/2})$
		1472	67 935					$n=4(^2E_{3/2})$ or $n=3(^2E_{3/2})+\nu_2$
1266	78 990	1440	69 445	1510	66 225			$n=2(^2E_{1/2})$
1245	80 320			1485	67 340			$n=2(^2E_{1/2})+\nu_2$
1205	82 990	1400	71 430	1455	68 730			$n=3(^2E_{1/2})$
1190	84 030							$n=3(^2E_{1/2})+\nu_2$
1170	85 470	1370	72 990					$n=4(^2E_{1/2})$
1140	87 720	1342	74 515					$n=4(^2E_{1/2})+\nu_2(?)$

corrections.[14] From the experimental point of view the CH_3I molecule is also interesting in view of its low gas phase ionization potential (the lowest values are $I_{g1}=9.49$ eV and $I_{g2}=10.11$ eV).[19] Thus the series of Wannier impurity states in inert matrices should be located at relatively low energies, and should be easily detected, provided they are amenable to experimental observation.

In Figs. 4, 5, 6, and 7 we display the absorption spectrum of CH_3I in solid neon, argon, krypton, and CF_4. In all the solid matrices, except solid Ne, we observe two series of transitions (see Table I) separated by an energy of 0.6–0.75 eV (see Table II). This energy difference which is close to the gas phase $^2E_{3/2}$–$^2E_{1/2}$ separation is assigned to the spin orbit splitting of the I atom. In solid Ne a splitting of 1.9 eV between the two series has been observed. This appreciable enhancement of the spin orbit coupling of an impurity in solid Ne (presumably due to large nonorthogonality corrections) has also been observed for Xe impurity states.[1] In solid Ne, Ar, and Kr Wannier impurity states up to $n=3$ or $n=4$ have been observed (see Table I). Another interesting feature of the present results (Table I) involves the observation of vibrational structure of the molecular Wannier states.

The CH_3I/CF_4 system (Fig. 7) provides a good example for a molecular impurity in a molecular host matrix. The lowest extravalence excitations $n=1$ ($^2E_{3/2}$) and $n=1$ ($^2E_{1/2}$) in this matrix exhibit a large blue shift (~1.5 eV) relative to the electronic origins in the gas phase. The $n=1$ ($^2E_{3/2}$) (1598 Å) and $n=1$ ($^2E_{1/2}$) (1455 Å) transitions exhibit two broad bands where all vibrational structure has been washed out due to phonon and relaxation line broadening in the CF_4 matrix. The spin orbit coupling in this matrix (0.76 eV) is somewhat higher than in the gas phase, the 25% increase (relative to the gas phase value) of the spin orbit coupling in the matrix is somewhat higher than the corresponding enhancement (~16%) of the spin orbit coupling of Xe in CF_4 (see Table I). As the nonorthogonality corrections to the spin orbit coupling[15] are very sensitive to molecular packing in

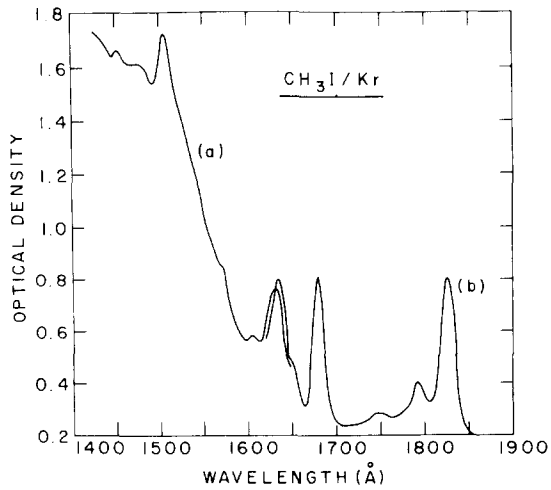

FIG. 6. Absorption spectrum of CH_3I in solid Kr. Gas phase composition 0.5% CH_3I in Kr. Deposition temperature 35°K. Curve (a), krypton-continuum light source. Curve (b), xenon-continuum light source.

the solid, it is not surprising that the CH_3I/CF_4 system exhibits somewhat larger spin orbit enhancement relative to Xe/CF_4. Higher Wannier states were not observed in the CH_3I/CF_4 system. Utilizing the data previously obtained by us[10] for Xe/CF_4 we have $G=2.5$ eV and $V_0\sim-0.1$ eV for solid CF_4. Taking $P_+\sim-0.5$ to -1.0 eV we estimate that the $n=2$ ($^2E_{3/2}$) state should be located somewhere in the range 8.3–8.8 eV (i.e., 1400–1500 Å). This transition overlaps the broad $n=1$ ($^2E_{1/2}$) band and was not observed by us. Another transition at 1330 Å (9.36 eV) was observed by us, which can be tentatively assigned to $n=2$ ($^2E_{1/2}$).

The CH_3I/Kr system (Table I and Fig. 6) exhibits the following features:

(a) Two Wannier series corresponding to $n=1$, 2, 3 ($^2E_{3/2}$) and $n=1$, 2, 3 ($^2E_{1/2}$) were observed.

(b) A vibration of 1100 ± 50 cm^{-1} was found for the $n=1$ and for the $n=2$ transitions in both series. This vibration corresponds to the ν_2 totally symmetric CH_3 deformation ($\nu_2=1090$ cm^{-1} in the gas phase)[20] which was also observed by Robin *et al.*[21] for CH_3I perturbed by nitrogen gas at high pressures.

(c) Spin orbit splitting of 0.59 eV between the $^2E_{3/2}$ and the $^2E_{1/2}$ series was observed which is close to the gas phase value (Table II).

The absorption spectrum of CH_3I/Ar (Table I and Fig. 5) exhibits the following characteristic features:

(a) Two long Wannier series, up to $n=4$, were observed for both $^2E_{3/2}$ and $^2E_{1/2}$ ionic core states.

(b) A relatively long vibrational progression characterized by a vibrational frequency of 960 ± 50 cm^{-1} is observed for the $n=1$ ($^2E_{3/2}$) transition, which is again attributed to the ν_2 vibration.

(c) The spin orbit splitting of 0.59 eV observed for the ^2E states in solid Ar is reasonable.

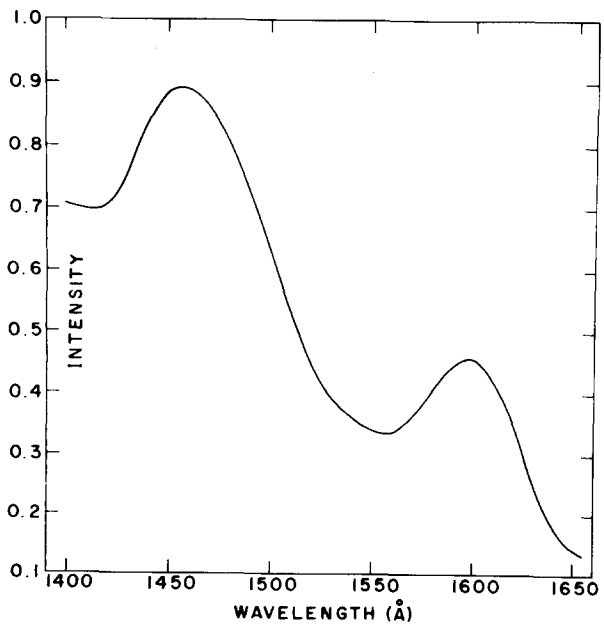

FIG. 7. Absorption spectrum of CH_3I in solid CF_4. Gas phase composition 0.5% CH_3I in CF_4. Deposition temperature 35°K.

TABLE II. Energy splitting between the $n=1$ states of methyl iodide and of Xe in solid matrices.

Matrix	Splitting between Xe $n=1(^2P_{3/2})$ and $n=1(^2P_{1/2})$ in eV	Splitting between CH_3I $n=1(^2E_{3/2})$ and $n=1(^2E_{1/2})$ in eV
Ne	2.20	1.88
Ar	1.31	0.59
Kr	1.21	0.59
CF_4	1.30	0.76
gas	1.13	0.595

The assignment for the CH_3I/Ne system (Fig. 4 and Table I) is fraught with difficulties in view of the large matrix effect on the spin orbit coupling. The lowest transition originating at 1705 Å (7.27 eV) and exhibiting a ν_2 vibrational progression of 1000 cm^{-1} (Table I) can be definitely assigned to the $n=1$ ($^2E_{3/2}$) state. The next impurity state is observed at 1475 Å (8.40 eV), i.e., 1.13 eV above the $n=1$ ($^2E_{3/2}$) state and would exhibit an appreciable matrix enhancement of the spin orbit coupling. However, we prefer to assign the 1475 Å (8.40 eV) transition to the $n=2$ ($^2E_{3/2}$) state, while the 1352 Å (9.17 eV) is attributed to the $n=1$ ($^2E_{1/2}$) state, because of the following reasons:

(a) The intensity ratio of the $n=2$ and $n=1$ transitions should be 1/8 for an ideal Wannier series and when central cell corrections are introduced this ratio can be reduced to $\sim1/3$.[12] The 1475 Å (8.40 eV) transition is weaker than the 1705 Å (7.27 eV) transition to the $n=1$ ($^2E_{3/2}$) state, which favors its assignment to the $n=2$ ($^2E_{3/2}$) excitation.

(b) Using the values $G=4.4$ eV and $V_0=0.6$ eV estimated for pure solid Ne,[22] and taking $P_+\sim-0.5$ eV, we estimate from Eq. (1) the energy of the $n=2$ ($^2E_{3/2}$) state to be located at 8.49 eV (68 000 cm^{-1}) which is very close to the 1475 Å band providing strong support to our assignment.

Some further comments concerning the CH_3I/Ne system (Table II) are in order. The $n=2$ ($^2E_{1/2}$) state located at 1266 Å (9.80 eV) is located $\sim$0.4 eV above the ionization limit of the Wannier series originating from the $^2E_{3/2}$ core. This state is metastable, decaying by autoionization.[23] Configuration interaction between the zero order $n=2$ ($^2E_{1/2}$) state and the conduction band states shifts the resonance to lower energies. A similar level shift is exhibited by the metastable $n=3$ ($^2E_{1/2}$) state which is located at 1205 Å (10.29 eV). Similar effects were previously exhibited by the Xe $n=2$ ($^2P_{1/2}$) and $n=3$ ($^2P_{1/2}$) impurity states in solid

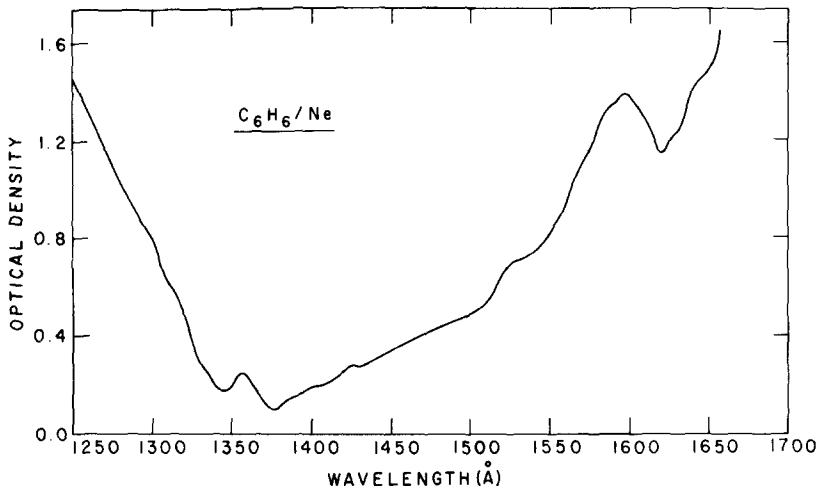

FIG. 8. Absorption spectrum of C_6H_6 in solid Ne. Gas phase composition 0.01% C_6H_6 in Ne. Deposition temperature 6°±2°K.

argon.[1] Thus, for the sake of a spectroscopic determination of the impurity band gap one has to utilize the data for the stable exciton states located below the lowest direct transition to the conduction band.

B. Benzene Impurity States

Extravalence excitations of benzene impurity states in solid Xe and Kr have been a subject of controversy. Katz *et al.*[6b] reported two transitions in C_6H_6/Kr (located at 59 100 and 62 200 cm^{-1}) and in C_6H_6/Xe (peaking at 57 500 and 60 300 cm^{-1}) which were assigned to the $n=1$ and to the $n=2$ Wannier states. These experimental data and their interpretation have been challenged by Angus and Morris[8b] on the basis of the following arguments:

(a) The second transition in C_6H_6/Xe reported by Katz *et al.*[6b] at 60 300 cm^{-1} was not observed by Angus and Morris[8b] who have suggested that the observation of this band in Katz's work is due to an experimental artifact originating from the *CI* emission line in the Kr continuum lamp. The second transition (62 200 cm^{-1}) in the C_6H_6/Kr system originally reported by Katz[6b] was also observed by Angus and Morris[8b] but no assignment was suggested by the latter authors.

(b) The photoemission thresholds determined by Angus and Morris[8b] ($F=8.08$ eV for C_6H_6/Xe and $F=8.25$ eV for C_6H_6/Kr) lead to an estimate of E_G [Eq. (2)] via the relation $F=E_G-V_0$. Utilizing the value $V_0=(-0.6\pm0.2)$ eV for solid Xe these authors estimate $E_G=7.5\pm0.3$ eV and [see Eq. (1)] $E_2=7.2\pm0.3$ eV for C_6H_6/Xe. Thus the 57 500 cm^{-1} (7.2 eV) transition in C_6H_6/Xe was assigned by Angus and Morris[8b] to the $n=2$ state, in contrast to the $n=1$ assignment advanced by Katz *et al.*[6b]

(c) The original assignment of Katz *et al.*[6b] was questioned[8b] as no higher members of the Wannier series were reported.

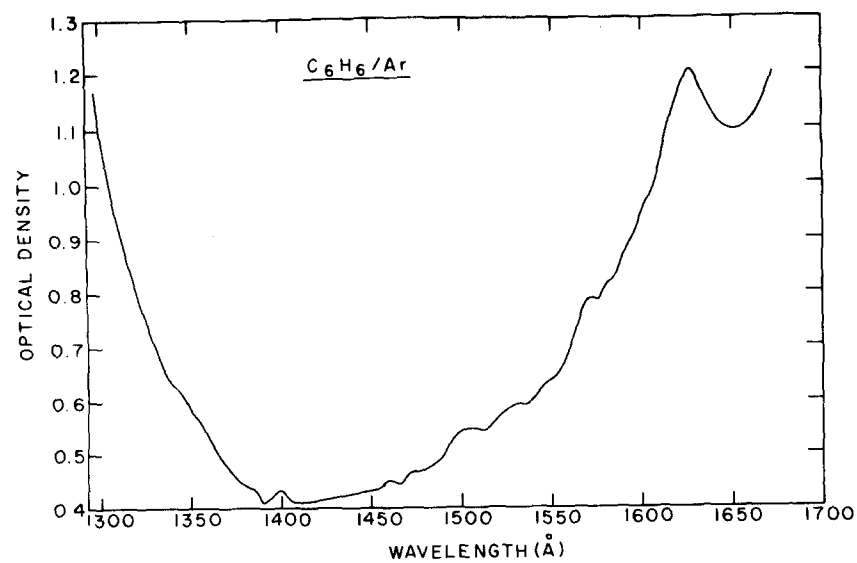

FIG. 9. Absorption spectrum of C_6H_6 in solid Ar. Gas phase composition 0.5% C_6H_6 in Ar. Deposition temperature 20°K.

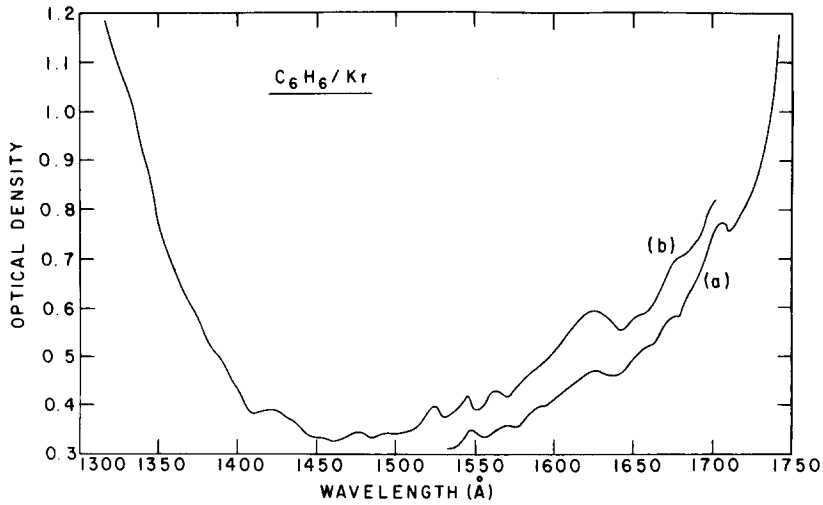

FIG. 10. Absorption spectrum of C_6H_6 in solid Kr. Gas phase composition 0.5% C_6H_6 in Kr. Deposition temperature 35°K. Curve (a), xenon continuum light source. Curve (b), krypton continuum light source.

In Figs. 8–12 we present the absorption spectra of C_6H_6 in solid Ne, Ar, Kr, Xe, and N_2, while the assignment of these spectra is given in Table III. The main new feature of our data is the observation of Wannier states up to $n=4$. The strongest absorption lines for C_6H_6/Xe and C_6H_6/Kr observed herein, using photoelectric detection, are in good agreement with the original photographic data of Katz *et al.*[6b] Our new data provide strong support for the original assignment[6b] proposed by Katz *et al.* because of the following reasons:

(a) The features of the C_6H_6/Xe spectrum obtained by us agree with the data of Katz *et al.* concerning the observation of the 60 400 cm^{-1} absorption band (see Fig. 5) which was not detected by Angus and Morris. This absorption spectrum was obtained by us using a Xe continuum lamp where the *CI* parasitic emission line is absent.

(b) Angus and Morris have used the value of $V_0=-0.6$ eV to estimate the energy of the $n=2$ state in C_6H_6/Xe. This value (within a fairly large uncertainty of ± 0.2 eV) was derived by Raz and Jortner[24] from the spectroscopic data of Haensel *et al.*[25] Photoelectric emission data[26] from pure solid Xe yield $V_0=-0.39$ eV. Utilizing $F=8.08$ eV and $V_0=-0.39$ eV for C_6H_6/Xe we estimate $E_2=7.5$ eV, which corresponds well to the $n=2$ assignment of the 60 400 cm^{-1} transition (Fig. 5 and Table II) in this system.

(c) The observation of a "long" Wannier series (up to $n=4$) reported herein provides a strong support to the original assignment of Katz *et al.*[6b] and to the present interpretation of the extravalence excitations of benzene impurity states.

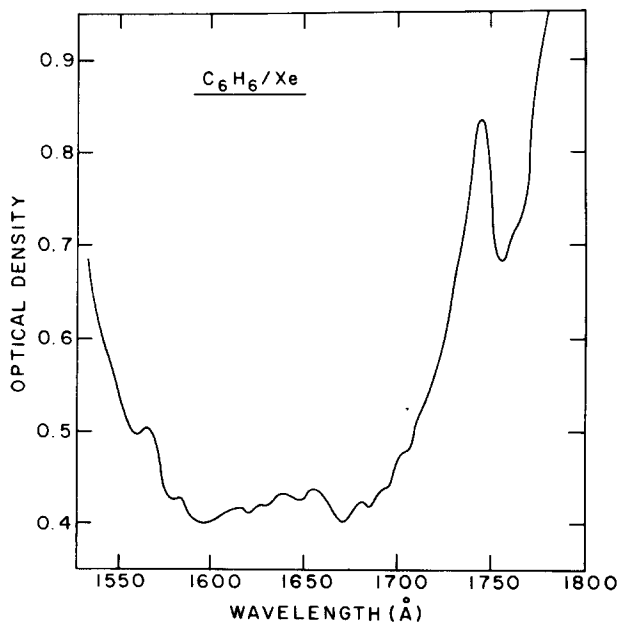

FIG. 11. Absorption spectrum of C_6H_6 in solid Xe. Gas phase composition 1.5% C_6H_6 in Xe. Deposition temperature 45°K.

The following comments concerning the experimental data (Table III) are in order:

(a) The molecular Wannier states of benzene in rare gas matrices exhibit a rather extensive vibrational structure. The most prominent vibration involves the ν_2 (920 cm^{-1} in the gas phase) totally symmetric mode. In C_6H_6/Xe and C_6H_6/Kr the doubly degenerate ν_{18} vibration (606 cm^{-1} in the gas phase) is exhibited being characterized by somewhat increased $\sim$700 cm^{-1} spacing. As has been previously discussed by Katz *et al.*,[6b] the appearance of this nontotally symmetric vibration originates from the effects of dynamic Jahn–Teller coupling in the $^2E_{2g}$ positive benzene ion core. As the matrix effects on the Jahn–Teller coupling are expected to be small, the Wannier states originating from a doubly degenerate $^2E_{2g}$ positive ion will exhibit the nontotally symmetric vibrational progression corresponding to the doubly degenerate e_{2g} mode.

(b) The observation of a long Wannier series of benzene in rare gas solids lead to a reliable estimate (see Sec. IV) of E_G [Eq. (1)]. The appearance of a weak but well defined absorption at the energy cor-

TABLE III. Energy levels of benzene impurity states in solid matrices.

Neon		Argon		Krypton		Xenon		
Wavelength Å	Energy cm^{-1}	Wavelength Å	Energy cm^{-1}	Wavelength Å	Energy cm^{-1}	Wavelength Å	Energy cm^{-1}	Assignment
1595	60 700	1625	61 540	1700	58 820	1745	57 310	$n=1$
1570	63 690	1595	62 690	1672	59 810	1710	58 480	$n=1+\nu_2$
				1655	60 420	1695	59 000	$n=1+\nu_2+\nu_{18}$
						1680	59 520	$n=1+2\nu_2$
1535	65 150	1570	63 690	1625	61 540	1655	60 420	$n=2$
		1550	64 520	1595	62 700			$n=2+\nu_2$
		1530	65 360					$n=2+2\nu_2$
1425	70 180	1505	66 450	1562	64 020	1632	61 280	$n=3$
		1475	67 800	1545	64 680	1615	61 920	$n=4$ or $n=3+\nu_{18}$
1355	73 780	1455	68 730	1525	65 570	1585	63 090	Eg (?)
		1430	69 930					

responding to E_G (Table III) is somewhat puzzling, as the density electron of states in the "free electron" like conduction band of these solids should increase steadily with increasing energy. It can be argued that this observed absorption results from the crowding of all the high Wannier states ($n>4$) near the onset of the direct transition to the conduction band.

(c) The line widths of the Wannier states of benzene in rare gas solids are sufficiently narrow (linewidths $\sim$500 cm^{-1}) to make these states amenable to experimental observation, in accord with theoretical arguments concerning weak electron-medium scattering in these solids. In solid N_2 (where the absorption of the matrix limits us to the study of the lowest extravalence excitation) we were able to observe a broad band (Fig. 12) which we assign to the $n=1$ state. The appreciable line broadening[27] of the $n=1$ state in C_6H_6/N_2 indicates strong electron medium scattering and correlates qualitatively with the low (10^{-2} cm^2 $V^{-1}\cdot sec^{-1}$) electron mobility in solid N_2.[28]

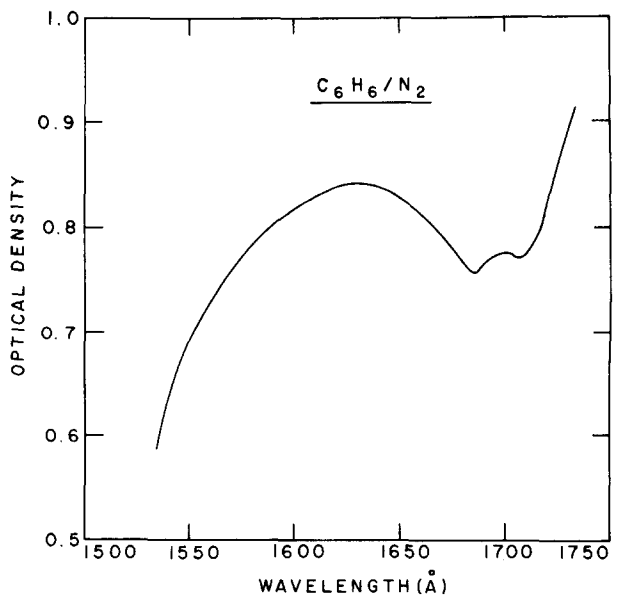

FIG. 12. Absorption spectrum of C_6H_6 in solid N_2. Gas phase composition 0.5% C_6H_6 in N_2. Deposition temperature 35°K.

C. Acetylene Impurity States

The absorption spectra of acetylene in Ne, Ar, Kr, and CF_4 (Figs. 13–16 and Table IV) exhibit the following features:

(a) The $n=1$ state was easily identified in all the matrices studied. The present results for C_2H_2/Ar and for C_2H_2/Kr are in good agreement with the original observations of Pysh *et al.*[5] and of Katz,[6a] except that we have not observed the sharp dip reported by Pysh, Rice, and Jortner[5] for C_2H_2/Ar at 1250 Å. This dip is apparently a spurious effect resulting from the use of a line source in the original work.[5]

(b) The $n=1$ state exhibits the totally symmetric ν_2 vibration. In solid Ar, Kr, and CF_4 the vibrational frequency is $\sim$1900 cm^{-1}, while in solid Ne a vibrational spacing of $\sim$1400 cm^{-1} was obtained. The corresponding gas phase frequency is $\nu_2=1781$ cm^{-1} (for the Rydberg state).[29] The intensity distribution for the 1375, 1350, and 1325 Å transitions in C_2H_2/Ne is similar to that observed for the $n=1$ transition in other matrices (see Fig. 7) so that the assignment of the former transitions is quite conclusive, in spite of the large reduction in the vibrational frequency in the Ne host matrix. The increase of the ν_2 frequency in Ar and Kr matrices is similar to the matrix effect on the totally symmetric vibration of C_2 in solid Xe.[30] The decrease of the ν_2 frequency in solid Ne may be due to matrix induced configurational change in this system.

(c) An interesting effect involves the relatively small linewidth ($\sim$300 cm^{-1}) of the electronic origin of the $n=1$ transition in solid Kr, while the line

TABLE IV. Energy levels of acetylene impurity states in solid matrices.

Neon		Argon		Krypton		CF_4		
Wavelength Å	Energy cm^{-1}	Wavelength Å	Energy cm^{-1}	Wavelength Å	Energy cm^{-1}	Wavelength Å	Energy cm^{-1}	Assignment
1375	72 730	1380	72 460	1428	70 030	1342	74 520	$n=1$
1350	74 070	1345	74 350	1392	71 840	1310	76 340	$n=1+\nu_2$
1325	75 470	1310	76 336	1355	73 800	1280	78 125	$n=1+2\nu_2$
1270	78 740	1295	77 220	1335	74 900	1255	79 680	$\tilde{E}+\tilde{F}$ states
1245	80 320	1270	78 740	1300	76 920	1235	80 970	$+\nu_2$
1225	81 630	1245	80 320	1270	78 740	1210	82 645	$+2\nu_2$
1200	83 330	1220	81 970			1190	84 030	$+3\nu_2$
1173	85 250							$n=2$(?)
1150	86 960							$n=2+\nu_2$
1130	88 500							$n=2+2\nu_2$(?)

broadening of the higher vibrational components in Kr, and all the $n=1$ transitions in Ne, Ar, and CF_4 is larger ($\sim$600 cm^{-1}). We attribute this effect to relatively weak electron phonon coupling in the Kr matrix, which should be treated by the theory of impurity line broadening, as was done for the Spolskii effect.[31]

A group of four absorption bands appear above the $n=1$ transition in all the four matrices studied by us (see Table IV). We cannot provide an unequivocal assignment for these transitions. The following possibilities were considered:

I. The bands are due to higher ($n\geq 2$) members of the Wannier series. This assumption is open to criticism because: (a) The intensities of these absorptions relative to the intensity of the $n=1$ transition are much higher than expected on theoretical grounds,[32] and higher than found for the relative intensity of the $n=2$ transition in the case of other impurities studied herein. (b) In C_2H_2/Ne the assignment of this group to the Wannier series contradicts the values of $E_{n=2}$ calculated from Eq. (1) according to the known value of G (4.4 eV).

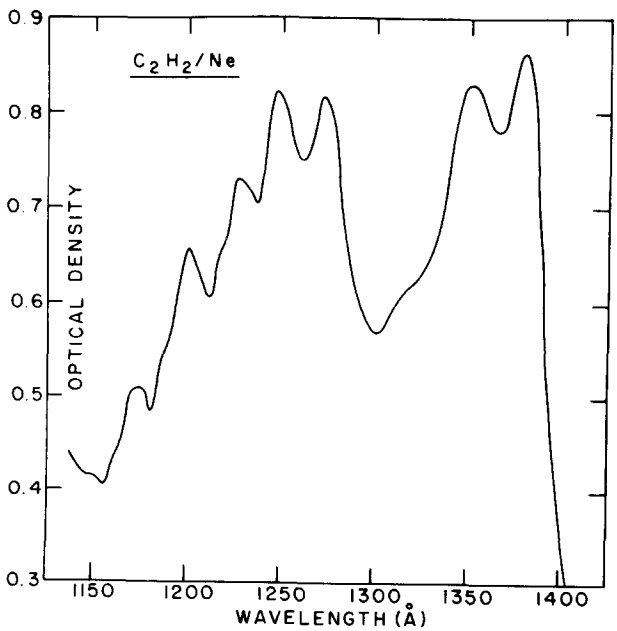

FIG. 13. Absorption spectrum of C_2H_2 in solid Ne. Gas phase composition 0.01% C_2H_2 in Ne. Deposition temperature 6°±2°K.

II. The bands correspond to the $n=1$ transition of a second Rydberg series (converging in the gas phase to 11.41 eV). The first member of this series has been identified in the gas phase by Price[33] and by Wilkinson[34] at 74 498 cm^{-1}. The lowest Rydberg transition of this second series is expected to exhibit a large blue spectral shift in all matrices. This shift increases in the order CF_4>Ne>Ar>Kr, which is the pattern observed for all other impurity states. The magnitude of the matrix shift for these four bands is then appreciably smaller than that observed for the other cases. Thus in solid Kr the blue shift of the 1335 Å band relative to the first member of the second Rydberg series is just 400 cm^{-1} as compared to the typical blue shift of 4000 cm^{-1} for the first Rydberg series in this matrix.

III. These absorptions originate from "intravalence" transitions to the excited E [35] and F [35] states in C_2H_2. The electronic origins of these transitions in the gas phase are located at 74 622 cm^{-1} and 74 747 cm^{-1}.[33,34] The fact that a matrix shift to higher energies was observed is in good agreement with Wilkinson's claim[29] that these states have a certain Rydberg character.

D. Ethylene Impurity States

The $N\rightarrow R$ transition of ethylene in the gas phase exhibits a doublet structure revealing the totally symmetric $\nu_2=1370$ cm^{-1} [36] progression simultaneously with an even change of the twisting $2\nu_4=472$ cm^{-1} mode. Katz and Jortner[6a] and Miron *et al.*[7] provided conclusive evidence for the observation of the lower Rydberg state of ethylene (or rather the $n=1$ im-

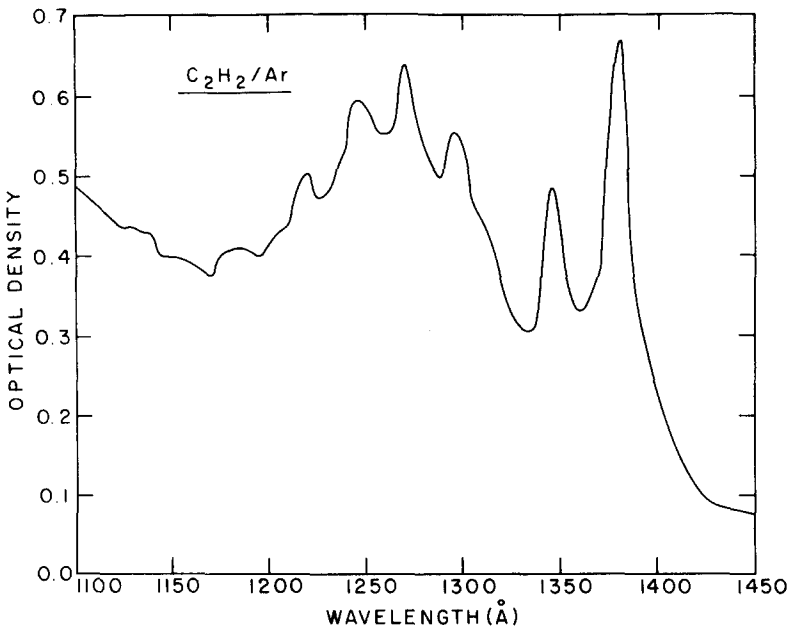

FIG. 14. Absorption spectrum of C_2H_2 in solid Ar. Gas phase composition 0.5% C_2H_2 in Ar. Deposition temperature 20°K.

purity state) in solid Kr. In Figs. 17–20 and in Table V we present our data for the absorption spectra of ethylene in solid Ne, Ar, Kr, and Xe, which exhibits the following features:

(a) The $n=1$ transition is easily identified in all the rare gas matrices.

(b) The $n=1$ transition exhibits the $\nu_2 \sim 1300$ cm^{-1} vibrational spacing. In solid Ne, Ar, and Kr the line broadening exceeds the vibrational spacing of the $2\nu_4$ mode, which could not be detected. In solid Xe we have observed a splitting of each of the vibrational components of the $n=1$ states which is assigned to the even change in the twisting mode.

(c) Higher Wannier states, corresponding to $n=2$ and $n=3$, were identified in Ne, Ar, and Kr matrices. These Wannier states exhibit the $\nu_2 \sim 1300$ cm^{-1} vibrational progression. In solid Xe we were unable to observe higher members of the Wannier series than the $n=2$ state in view of the absorption by the host matrix.

(d) The observation of the $n=2$ state of C_2H_4/Ar at 1440 A confirms the tentative assignment of the $n=2$ state of ethylene in liquid argon at 1480 Å, reported by Miron *et al.*[7] In liquid argon vibrational structure of the $n=2$ state was completely washed out (due to line broadening) while in the solid the vibrational structure could be resolved.[7] A similar situation

TABLE V. Energy levels of ethylene impurity states in solid matrices.

Neon		Argon		Krypton		Xenon		
Wavelength Å	Energy cm^{-1}	Wavelength Å	Energy cm^{-1}	Wavelength Å	Energy cm^{-1}	Wavelength Å	Energy cm^{-1}	Assignment
1565	63 900	1580	63 290	1620	61 730	1655	60 420	$n=1$
						1645	60 790	$n=1+2\nu_4$
1535	65 150	1547	64 640	1590	62 890	1625	61 540	$n=1+\nu_2$
						1615	61 920	$n=1+\nu_2+2\nu_4$
1510	66 225	1517	65 920	1562	64 020	1593	62 774	$n=1+2\nu_2$
1480	67 570	1485	67 340			1565	63 900	$n=1+3\nu_2$
1405	71 170							
1380	72 460							
1360	73 530							
1330	75 190	1440	69 440	1475	67 800	1565	63 900	$n=2$
1300	76 900	1420	70 420	1443	69 300			$n=2+\nu_2$
		1395	71 680	1430	69 930			$n=3$
		1370	72 990	1400	71 430			$n=3+\nu_2$ or $E_g(?)$
		1330	75 190	1383	72 310			$E_g+\nu_2(?)$

prevails for the $n=2$ excitation of ethylene in solid and liquid rare gases.

Finally we would like to admit that we were unable to provide an assignment for the absorption in the range 1405–1330 Å of ethylene in solid neon.

IV. DISCUSSION

A. Binding Energies for Molecular Wannier States

The identification of highly excited Wannier states ($n\geq 2$) originating from a molecular positive ion in

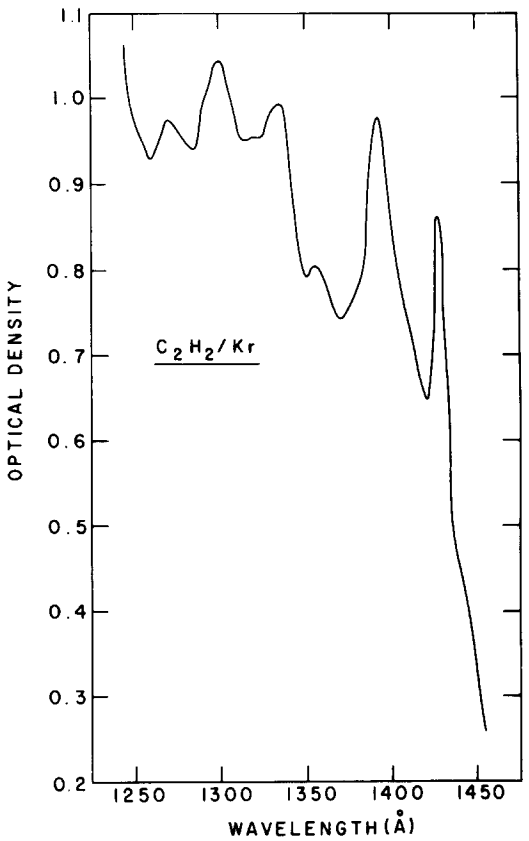

FIG. 15. Absorption spectrum of C_2H_2 in solid Kr. Gas phase composition 0.5% C_2H_2 in Kr. Deposition temperature 35°K.

the spectra of methyl iodide, benzene, and ethylene in rare gas solids, enables us to utilize Eq. (1) for estimates of the impurity binding energies. The plots of E_n vs n^{-2} corresponding to the electronic origins of the molecular Wannier states (Fig. 21) are linear, providing a strong qualitative support for our spectroscopic assignments. In Table VI, we present the values of the impurity energy gaps and the excited state binding energies as obtained for different molecular impurities in rare gas solids. With the use of the experimental data for the dielectric constant, the effective electronic mass in the matrix conduction band was estimated. Obviously, the G and the m^* values are an intrinsic property of the host matrix,

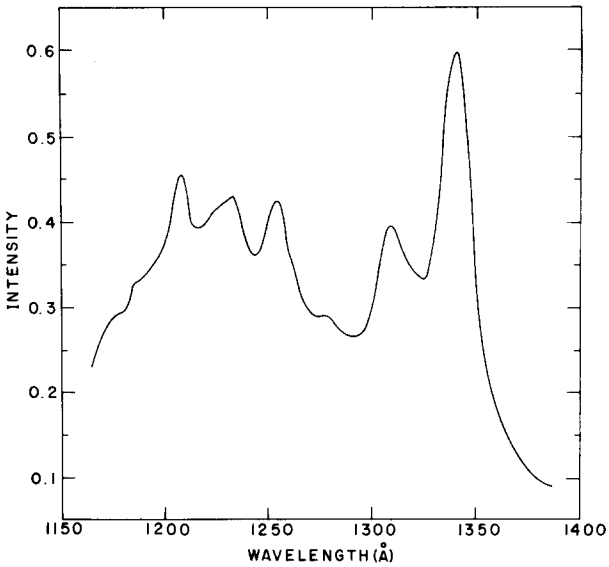

FIG. 16. Absorption spectrum of C_2H_2 in solid CF_4. Gas phase composition 0.5% C_2H_2 in CF_4. Deposition temperature 35°K.

being independent of the nature of the molecular (or atomic) impurity. It is comforting to notice (see Table VI) that our G values calculated for different impurities in a given host matrix are practically constant, being equal to previous estimates obtained for Xe atomic impurity in that matrix.[1] This result provides strong support for the basic theoretical assumption that high extravalence excitations of molecular impurity states do not exhibit any relation to the Rydberg states of the "isolated" molecule, and can be adequately described by the Wannier model.

B. Molecular Ionization Potentials in Solid Rare Gases

The molecular impurity energy gaps (Table VI) combined with the gas phase ionization potentials

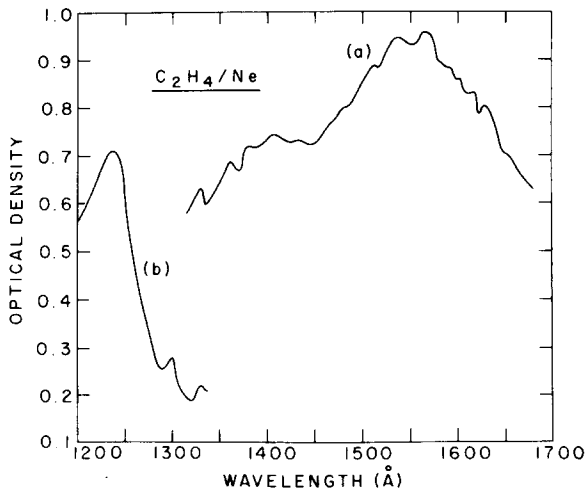

FIG. 17. Absorption spectrum of C_2H_4 in solid Ne. Gas phase composition 0.01% C_2H_4 in Ne. Deposition temperature 6°±2°K. Curve (a), krypton continuum light source. Curve (b), argon continuum light source.

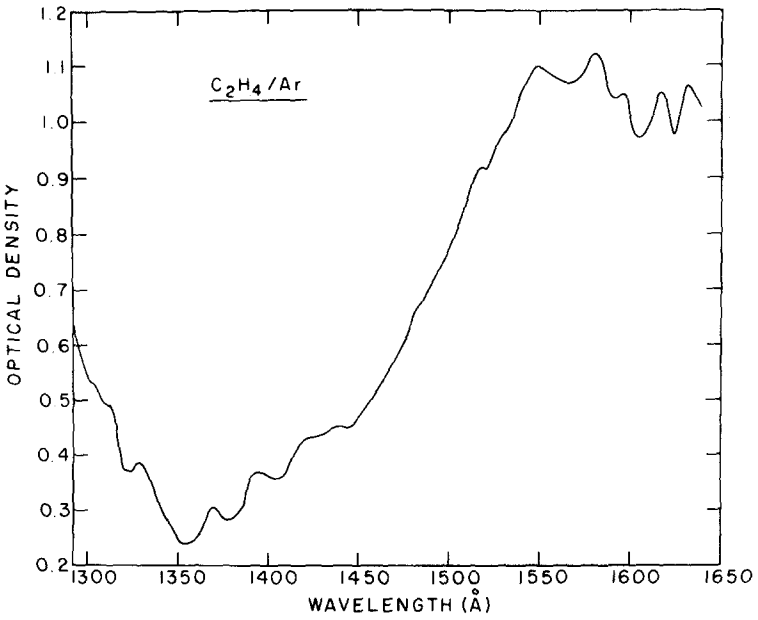

FIG. 18. Absorption spectrum of C_2H_4 in solid Ar. Gas phase composition 0.6% C_2H_4 in Ar. Deposition temperature 20°K.

[see Eq. (3)] lead to a reliable estimate of $(P_+ + V_0)$. The energies of the bottom of the conduction band are available from adiabatic electron injection experiments[37] (for liquid Ar which should be close to V_0 for solid Ar), from photoemission data[26] (for solid Xe), and from spectroscopic data of atomic impurity exciton states and x-ray excitons (for solid Ne, Ar, Kr, and Xe).[1,2,25] Utilizing these V_0 data we estimate the positive ion polarization energies P_+ (see Table VII). These P_+ values are determined by the host matrix and by the molecular impurity, increasing from Ne to Xe, as expected.

C. Spectral Shifts of the $n=1$ State

It is now well established that the lowest extravalence excitations of molecular impurities in atomic and in molecular host matrices exhibit a large blue spectral shift relative to the lowest Rydberg state of the isolated molecule.[5–8] Adopting the treatment based on the modified tight binding scheme for the intermediate $n=1$ excited state, we present in Table VII these spectral shifts for the systems studied herein. From the experimental point of view the blue shifts of the $n=1$ molecular impurity states are given in the order

$$Xe<Kr<Ar<Ne<CF_4.$$

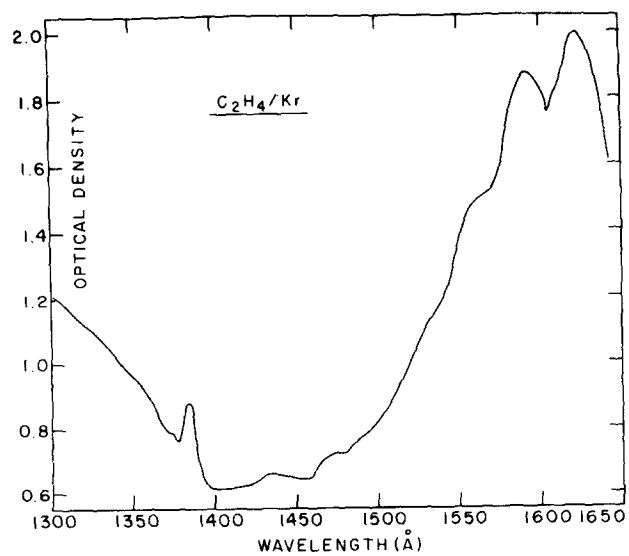

FIG. 19. Absorption spectrum of C_2H_4 in solid Kr. Gas phase composition 1.0% C_2H_4 in Kr. Deposition temperature 35°K.

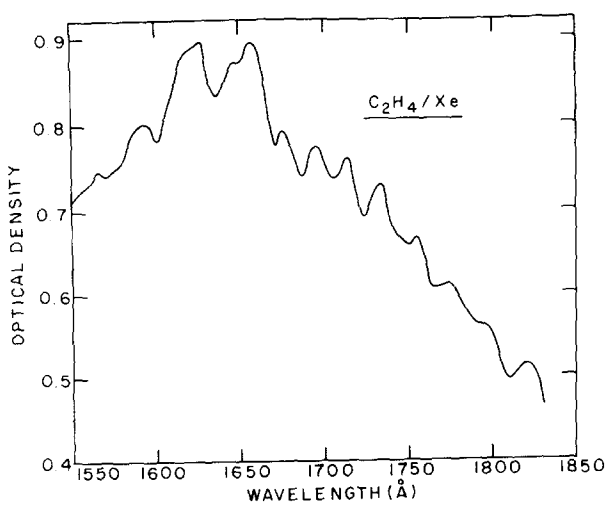

FIG. 20. Absorption spectrum of C_2H_4 in solid Xe. Gas phase composition 0.5% C_2H_4 in Xe. Deposition temperature 45°K.

TABLE VI. Energetic data for large radius impurity states of CH_3I, C_2H_4, and C_6H_6 in rare gas solids (all energies in eV, m^* expressed in units of the electron mass).

	Ne matrix	Ar matrix	Kr matrix	Xe matrix	Guest molecule
E_g	10.43	9.13	8.88	8.14	C_2H_4
G	4.4	2.10	1.88	0.88	$I_g=10.50$ eV
m^*	0.5	0.43	0.45	0.32	
$P_+ + V_0$	−0.08	−1.38	−1.63	−2.37	
V_0	0.60	−0.30	−0.62	−0.39	
P_+	−0.68	−1.08	−1.01	−1.98	
E_g	9.51	8.58	8.13	...	CH_3
G	4.4	2.2	−2.10	...	$I_g=9.49$ eV
m^*	0.5	0.45	0.50	...	
$P_+ + V_0$	0.02	−0.91	−1.36	...	
V_0	0.60	−0.3	−0.62	...	
P_+	−0.62	−0.6	−0.74	...	
E_g	9.19	8.51	8.18	7.75	C_6H_6
G	4.45	2.40	2.12	1.00	$I_g=9.24$ eV
m^*	0.5	0.49	0.51	0.37	
$P_+ + V_0$	−0.06	−0.74	−1.07	−1.50	
V_0	0.60	−0.3	−0.62	−0.39	
P_+	−0.66	−0.44	−0.45	−1.13	
E_g	12.15	10.54	10.40		Xe
G	4.4	2.4	1.72		$I_g=12.13$ eV
m^*	0.5	0.5	0.6		
$P_+ + V_0$	0.02	−1.59	−1.73		
V_0	0.6	−0.3	−0.62		
P_+	−0.58	−1.29	−1.11		

These matrix shifts and their order provide a very useful criterion for the identification of the intermediate $n=1$ state in solids. It is very difficult to adopt Frenkel's tight binding scheme to provide a quantitative description of these spectral shifts. In particular, the large blue shift observed for solid CF_4 is quite puzzling.

We have previously pointed out[10] that the energy levels of the $n=1$ Xe atomic impurity states in atomic and molecular matrices can be adequately described in terms of a linear dependence of the central cell correction [Eq. (5)] on the exciton binding energy.[10,12] The central cell corrections for molecular impurities are summarized in Table VIII. In Fig. 22 we display the central cell corrections for the $n=1$ state of benzene and ethylene and Xe impurities which exhibit a reasonably accurate linear dependence of ΔE_c on G. Thus the approximate linear dependence

$$\Delta E_c=\alpha+\beta G, \tag{6}$$

where the constants α and β are determined by the nature of the impurity, seems to be of general applicability. Relation (6) is qualitatively consistent with the theoretical estimates of Harmenson and Phillips[12,38] (for Xe impurity states), which demonstrate that the deviations from the Wannier model, i.e., the central cell corrections, increase with increasing the excited state binding energy.

V. CONCLUDING REMARKS

We were able to provide new experimental information concerning the following features of highly excited molecular impurity states in rare gas and in

TABLE VII. Spectral shifts of the $n=1$ transition of molecular impurities relative to the electronic origin of the lower Rydberg state in the gas phase.

Impurity\Matrix	Xe cm^{-1}	Kr cm^{-1}	Ar cm^{-1}	Ne cm^{-1}	CF_4 cm^{-1}	N_2 cm^{-1}
CH_3I	...	5095	6480	8950	12 880	...
C_6H_6	1400	2920	5640	6800	...	5520
C_2H_4	2850	4160	5720	6330	...	...
C_2H_2	...	4210	6650	6910	8 700	...

TABLE VIII. Central cell corrections in various matrices (in eV).

D_2	CF_4	Ne	Ar	Kr	Xe	Matrix/Guest
0.75	1.09	2.34	1.04	0.55	0.06	Xe[a]
...	...	1.74	1.36	0.64	...	C_2H_2
...	...	1.90	0.79	0.66	0.21	C_2H_4
...	...	3.00	1.55	1.24	0.36	C_6H_6
...	...	2.16	0.59	0.63	...	CH_3I

[a] Adopted from Ref. 10.

molecular host matrices:

(a) The position of the lowest extravalence molecular excitation in solid matrices, which exhibits a large blue shift relative to the gas phase can be properly rationalized in terms of central cell corrections to the $n=1$ Wannier state. These central cell corrections are determined by the exciton binding energy.

(b) Molecular Wannier impurity states have been identified in molecular host matrices such as solid CF_4 and solid N_2. These results provide an extension of previous work which concentrated on rare gas host matrices and yield some further information concerning line broadening of Wannier impurity states.

(c) Conclusive experimental evidence has been obtained for the observation of high $n\geq 2$ Wannier impurity states originating from a molecular positive hole in solid matrices.

(d) The observation of the hydrogeniclike series of molecular Wannier states in atomic and molecular host matrices yields a reliable estimate of the impurity gap E_G (i.e., the ionization potential in the dense medium). Equation (3) then provides us with the values of $(P_+ + V_0)$, and the utilization of our previous estimates for V_0 [22] yields the medium polarization energy for different molecular ions in various host matrices. Thus, spectroscopic information is obtained pertaining to one photon ionization processes of molecular impurity states in solids.

Several interesting theoretical and experimental problems in this field have still to be elucidated.

A. The Absence of the Liehr Splitting for $n=1$ State

It is well known that the Rydberg states of isolated large molecules exhibit several series, characterized by different quantum defects, which converge to the same ionization limit. This phenomenon has been interpreted by Liehr in terms of deviations from the point charge potential of the positive ion core.[39] The Liehr splitting between members of different series characterized by the same principal quantum number, n, decreases with increasing n. A similar effect has to be observed for the lowest molecular Wannier states in a dense medium, although the magnitude of the Liehr splitting has to be reduced (relative to the splitting in the lowest Rydberg state of the free molecule) due to dielectric screening effects. Our experimental results for benzene and ethylene (which exhibit the Liehr splitting in the gas phase)[36,40] do not exhibit this splitting in dense media. This problem calls for a theoretical treatment of the magnitude of the Liehr splitting for impurity states.

B. Metastable Impurity States

Excited impurity states above the direct threshold of the conduction band are metastable, and will decay by autoionization. We have observed such states for CH_3I in rare gas solids where the high $n(^2E_{1/2})$ states are located above the onset of the $(^2E_{3/2})$ conduction band. We were unable to identify metastable molecular impurity states in the other molecular systems studied by us which could be due to excitation from lower lying valence orbitals. The main difficulty in observing these states originates from the presence of broad absorption continua in the vacuum ultraviolet spectra (see V.C).

C. Broad Background Continua

The extravalence excitations of molecular impurity states are often superimposed on broad structureless continua. In the case of the ethylene spectrum this continuous absorption is quite well understood, originating from the photodissociation to the limit of the $\pi \rightarrow \pi^*$ transition. The continua exhibited in the spectra of methyl iodide and benzene impurities observed by us originate probably from molecular photodissociation and/or predissociation. Their study will be of interest although such an investigation is by no means limited to dense media. The presence of these molecular continua prevent the observation of interband transitions (to the conductive band) for molecular impurity states.

TABLE IX. Linewidth of the $n=1$ impurity state of various molecules in solid matrices.

Nitrogen cm^{-1}	CF_4 cm^{-1}	Neon cm^{-1}	Argon cm^{-1}	Krypton cm^{-1}	Xenon cm^{-1}	Matrix/Guest
...	...	...	...	1010	620	C_2H_4
3580	...	2760	1240	1070	570	C_6H_6
...	1250	1590	760	345	...	C_2H_2
...	2320	1140	760	550	...	CH_3I

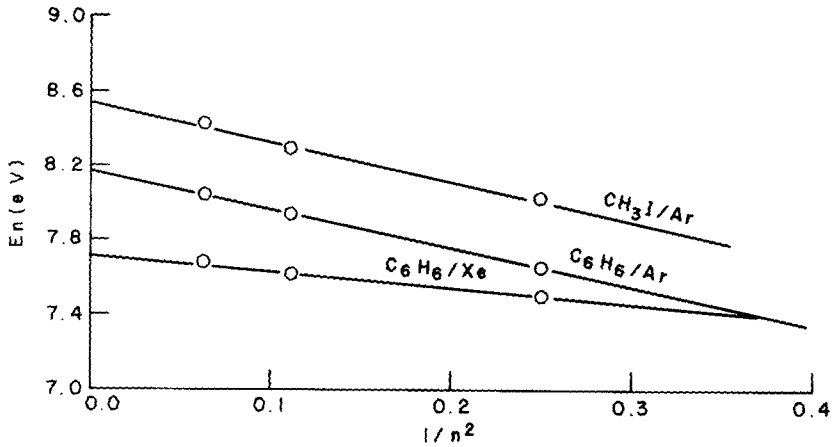

FIG. 21. Plots of En vs n^{-2} for molecular impurity states in rare gas solids.

D. Line Broadening of Wannier Molecular Impurity States

The qualitative theoretical treatment[27] of the linewidths of large radius extravalence excitations in a dense medium provided an impetus for the experimental study of these states. It is now well established that Wannier impurity states are amenable to experimental observation in molecular solids where electron–molecule scattering is weak, whereupon the line broadening is not prohibitive for the experimental observation of these states. This approach[27] does not apply for the intermediate type $n=1$ Wannier states. To get some idea concerning this problem we have assembled in Table IX the linewidths of the $n=1$ state for molecular impurities, and compared them with available data for Xe atomic impurity states. In view of a possible contribution of "trivial" broadening effects such as a distribution of trapping sites and the Liehr splitting the data in Table IX provide an upper limit for the linewidths. These linewidths should be interpreted in terms of several contributions: (a) conventional phonon broadening based on the displacements of the medium normal modes between the ground and excited states, (b) intramolecular electronic relaxation to lower lying intravalence molecular states. As is known from gas phase spectroscopic data[41] the interstate coupling between intravalence and extravalence excitations is weak and this line broadening effect is not appreciable. The role of phonon broadening mechanism on the $n=1$ state can be elucidated from the temperature dependence of the linewidths as previously performed for Xe impurity states.[42] Turning now our attention to higher

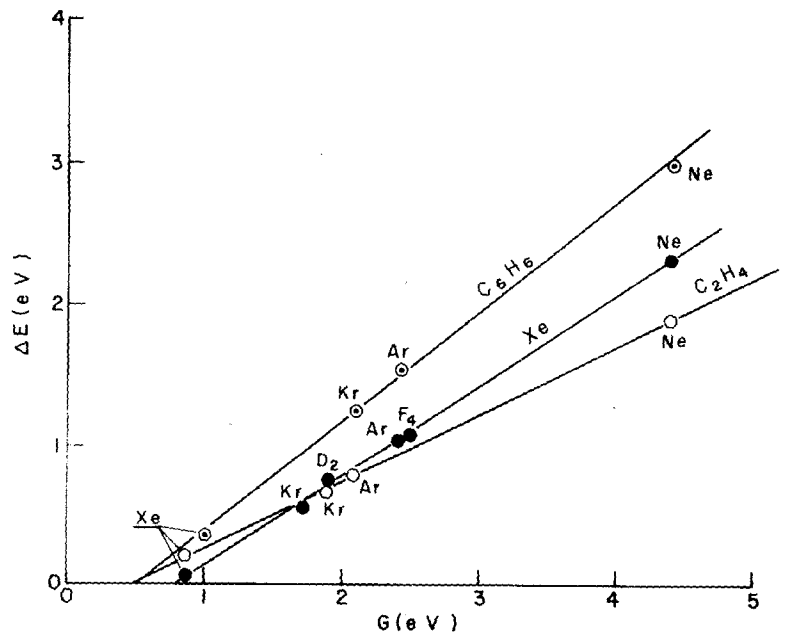

FIG. 22. Central cell corrections $\Delta E_c = E_1^{\text{exptl}} - E_1^{\text{calc}}$ for the $n=1$ impurity state of molecular impurities in inert matrices vs the exciton binding energy G.

large radius (stable) molecular Wannier states several contributions to the line broadening have to be considered: (a) phonon broadening, (b) intramolecular electronic relaxation, which, as in the case of the $n=1$ state, is of minor importance, (c) electron scattering in the excited state, (d) electronic relaxation between the high Wannier states and lower Wannier states, cascading nonradiatively to the $n=1$ state. A complete treatment of this problem will be of considerable interest.

[1]G. Baldini, Phys. Rev. A **137,** 508 (1965).
[2]J. Y. Roncin, V. Chandrasckharan, N. Damany, and M. B. Vodar, J. Chem. Phys. **60,** 1212 (1963).
[3]E. Boursey and J. Y. Roncin, Phys. Rev. Lett. **26,** 308 (1971).
[4]A. Gedanken, B. Raz, and J. Jortner, Chem. Phys. Letters **14,** 326 (1972).
[5]E. Pysh, S. A. Rice, and J. Jortner, J. Chem. Phys. **43,** 2997 (1965).
[6](a) B. Katz and J. Jortner, Chem. Phys. Lett. **2,** 437 (1968). (b) B. Katz, M. Brith, B. Sharf, and J. Jortner, J. Chem. Phys. **50,** 5195 (1969).
[7]E. Miron, B. Raz, and J. Jortner, J. Chem. Phys. **56,** 5265 (1972).
[8](a) J. G. Angus and G. C. Morris, Mol. Cryst. Liq. Cryst. **11,** 257 (1970). (b) J. G. Angus and G. C. Morris, Mol. Cryst. Liq. Cryst. **11,** 309 (1970).
[9]J. Y. Roncin, N. Damany, and B. Vodar, Chem. Phys. Lett. **3,** 197 (1969).
[10]A. Gedanken, B. Raz, and J. Jortner, Chem. Phys. Lett. **14,** 172 (1972).
[11]W. Kohn, *Solid State Physics*, edited by D. Turnbull and F. Seitz (Academic, New York, 1957), Vol. 5, p. 258.
[12](a) J. Hermanson, Phys. Rev. **150,** 660 (1967). (b) J. Hermanson and J. C. Phillips, Phys. Rev. **150,** 652 (1967).
[13]S. Webber, S. A. Rice, and J. Jortner, J. Chem. Phys. **42,** 1907 (1965).
[14]A. Gold and R. S. Knox, Phys. Rev. **113,** 834 (1959).
[15]B. Raz, J. Magen, and J. Jortner, Vacuum **19,** 571 (1969).
[16]G. Baldini, Phys. Rev. **128,** 1562 (1962).
[17](a) O. Schnepp and K. Dresler, J. Chem. Phys. **33, 49** (1960). (b) M. Skibowski (unpublished results).
[18]S. R. Scharber, Jr. and S. E. Webber, J. Chem. Phys. **55,** 3985 (1971).
[19]W. C. Price, J. Chem. Phys. **4,** 539 (1936).
[20]G. Herzberg and G. Scheibe, Z. Phys. Chem. B **7,** 390 (1930).
[21]M. B. Robin and N. A. Kuebler, J. Mol. Spectrosc. **33,** 274 (1970).
[22]B. Raz and J. Jortner, Chem. Phys. Lett. **9,** 222 (1971).
[23]Another parallel nonradiative decay channel of the $n(^2E_{1/2})$ state may involve electronic relaxation to lower lying $n(^2E_{3/2})$ bound states.
[24]B. Raz and J. Jortner, Chem. Phys. Lett. **4,** 155 (1969).
[25]R. Haensel, G. Keitel, E. E. Koch, M. Skibowsky, and P. Schreiber, Phys. Rev. Lett. **23,** 1160 (1969).
[26]F. J. O'Brien and K. J. Teegarden, Phys. Rev. Lett. **17,** 919 (1966).
[27]S. A. Rice and J. Jortner, J. Chem. Phys. **44,** 4470 (1966).
[28]R. J. Loveland, P. G. LeComber, and W. E. Spear, Phys. Rev. B **6,** 3121 (1972).
[29]P. G. Wilkinson, J. Mol. Spectrosc. **2,** 387 (1958).
[30]M. McCarty and G. W. Robinson, Mol. Phys. **2,** 415 (1959).
[31]J. L. Richards and S. A. Rice, J. Chem. Phys. **54,** 2014 (1971).
[32]R. J. Elliot, Phys. Rev. **108,** 1384 (1957).
[33]W. C. Price, Phys. Rev. **47,** 444 (1935).
[34]P. G. Wilkinson, J. Mol. Spectrosc. **2,** 387 (1958).
[35]G. Herzberg, *Electronic Spectra and Electronic Structure of Polyatomic Molecules* (Van Nostrand, Princeton, N. J., 1967).
[36](*a*) P. G. Wilkinson, Can. J. Phys. **34,** 643 (1956).(*b*) R. S. Mulliken and P. G. Wilkinson, J. Chem. Phys. **23,** 1825 (1956).
[37]B. Halpern, J. Lekner, S. A. Rice, and R. G. Gomer, Phys. Rev. **156,** 351 (1967).
[38]J. Hermanson and J. C. Phillips, Phys. Rev. **150,** 652 (1966).
[39]A. Liehr, Z. Naturforsch. A **11,** 752 (1956).
[40]P. G. Wilkinson, Can. J. Phys. **34,** 596 (1956).
[41]M. Bixon and J. Jortner, J. Chem. Phys. **48,** 715 (1968).
[42]Z. Ophir, B. Raz, and J. Jortner (unpublished).